DOI: 10.1002/ejic.200700862

Syntheses, Crystal Structures, and Optical Properties of Metal Complexes with 4′,5′-Diaza-9′-(4,5-disubstituted-1,3-dithiol-2-ylidene)fluorene Ligands

Qin-Yu Zhu,[a] Wen Lu,[a] Yong Zhang,[a] Guo-Qing Bian,[a] Jing Gu,[a] Xiao-Min Lin,[a] and Jie Dai*[a]

Keywords: Metal complexes / Crystal structure / Optical properties / Dithioles / Fluorenes

Four complexes with 4′,5′-diaza-9′-[4,5-bis(methylthio)-1,3-dithiol-2-ylidene]fluorene (L^1) or 4′,5′-diaza-9′-[4,5-bis(ethylthio)-1,3-dithiol-2-ylidene]fluorene (L^2) were synthesized. The complexes $[Co(L^1)_2Cl_2]·2CH_3OH$ (**1**), $[Cu(L^2)_2Cl_2]·CH_3OH·0.5CH_2Cl_2$ (**3**), and $[Cu(L^2)_2Br_2]·CH_3OH$ (**4**) adopt a *trans* configuration and the compound $[Cd(L^1)_2(NO_3)_2]$ (**2**) is a *cis* structure. Short S···S, C···C, and C···S contacts were found to be important in the molecular packing. Both the solution and solid-state electronic spectra show a redshift in the intramolecular CT bands when forming metal complexes. This intramolecular charge transition in the solid state is enhanced relative to that in solution. Their third-order nonlinear optical properties of compounds **1**–**4** were studied, and the results reveal that these complexes exhibit negative γ values (about 10^{-30}) and are self-defocusing samples. These γ values are comparable to those of the known cluster compounds. The *trans* coordination of the two ligands to the metal center would be beneficial to the NLO properties.
(© Wiley-VCH Verlag GmbH & Co. KGaA, 69451 Weinheim, Germany, 2008)

Introduction

The demand for photoactive molecular materials is continuously on the increase, because of their possible use as photodetectors, photoswitches, solar cells, and photodiodes. In particular, the search for multifunctional materials combining magnetism[1] or conductivity[2] with nonlinear optical (NLO) properties is currently a field of great interest.[3] Most devices exploit inorganic materials, as they can often be easily fabricated as ordered crystals, whose photovoltaic and electronic properties are generally superior to those of amorphous phases, but the multiple-frequency susceptibility of such inorganic NLO devices is not big enough. Also, organic thin films guarantee interesting properties, such as, flexibility in synthesis, ease of processability, and lower susceptibility to lattice impurities.[4,5] Bearing the properties of organic compounds and the diversity of coordination structures, metal complexes are expected to be new materials possessing good properties of the NLO compounds that have been the subject of intense investigation.[6] It is noted that when transition metals coordinate with functionalized organic ligands, the incorporation of d electrons into the conjugated organic system greatly enhances its hyperpolarizability and nonlinear susceptibility.[7]

On the other hand, metal dithiolene complexes have been the matter of active research owing to their relevance to biology, catalysis, and material science.[8] A large number of metal dithiolene derivatives with fluorene moieties have been reported.[9,10] For example, Hosseini and coworkers reported the structures of complexes with dithiolene ligands appended with a 4,5-diazafluorene moiety.[9] Vicente and coworkers studied the structures and the luminescent properties of metal complexes with similar ligands.[10] We also described the structures and catalysis or fluorescence properties of several complexes with the title ligands.[11] Recently, some metal–dithiolene complexes possessing good third-order NLO properties have been reported.[12] However, to our best knowledge, there are no reports on the third-order nonlinearity of metal complexes with dithiolene ligands appended with a fluorene moiety. The title ligands used in this work are such systems that include not only an electron-donor sulfur-rich moiety but also a conjugated electron-withdrawing bipyridine moiety, which meet the needs of the compounds possessing NLO properties and good coordination abilities. Therefore, we have continuously been interested in the title ligands (Scheme 1), and we investigated the solid state chemistry and the third-order NLO properties of the corresponding complexes. In this pa-

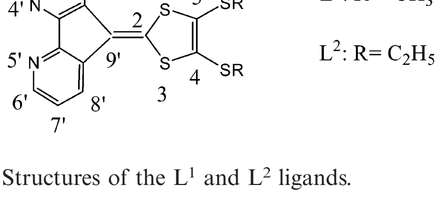

Scheme 1. Structures of the L^1 and L^2 ligands.

---

[a] Department of Chemistry, Key Laboratory of Organic Synthesis of Jiangsu Province, Suzhou University,
P. O. Box 174, Suzhou 215123, China
E-mail: daijie@suda.edu.cn

per, we present the syntheses, crystal structures, and third-order susceptibilities, χ^3, of four transition-metal complexes with the title ligands, $[Co(L^1)_2Cl_2]·2CH_3OH$ (**1**), $[Cd(L^1)_2(NO_3)_2]$ (**2**) (L^1 = 4′,5′-diaza-9′-[4,5-bis(methylthio)-1,3-dithiol-2-ylidene]fluorene, $[Cu(L^2)_2Cl_2]·CH_3OH·0.5CH_2Cl_2$ (**3**) and $[Cu(L^2)_2Br_2]·CH_3OH$ (**4**) {L^2 = 4′,5′-diaza-9′-[4,5-bis(ethylthio)-1,3-dithiol-2-ylidene]fluorene}.

Results and Discussion

General Discussion

The complexes with bipyridine and 1,10-phenanthroline ligands have been widely researched, but they are not good candidates for third-order nonlinear optical materials in view of the fact that third-order NLO molecules usually possess large π systems with rich electron density. The ligands L^1 and L^2 have a bipyridine moiety, but they also posses a dimethylthio-1,3-dithiole unit, which is a sulfur-rich moiety with high electron density. The physical and chemical properties of these ligands and their complexes may be different from those of the phenanthroline and bipyridine units, because of the change in the electron density and the relative levels of the π orbitals. The ligands were synthesized by using a modified literature procedure (see the Experimental Section). Compounds **1**–**3** were synthesized in a similar procedure, by slowly evaporating the reaction mixture at room temperature. However, crystals of compound **4** were obtained by a diffusion method because of its lower solubility. Coordination of the metal causes the central ν(C=C) band of the ligands in the IR spectra of complexes **1**–**4** to be clearly shifted to a lower energy and the S–C–S vibrations are enhanced relative to those of the corresponding free ligands.

Structural Descriptions

$[Co(L^1)_2Cl_2]·2CH_3OH$ (1)

Complex **1** crystallizes in a monoclinic system with four molecules and two solvent molecules (MeOH) in a unit cell. The X-ray crystal structure of compound **1** is shown in Figure 1 and selected bond lengths and bond angles are listed in Table 1. Disorders were found for the C and O atoms of the two solvent molecules. In the crystal structure of **1**, the cobalt atom is symmetrically chelated by four nitrogen atoms from two L^1 ligands, forming a quasiplanar structure including the cobalt(II) ion with a mean deviation of 0.036 Å. Perpendicular to the plane there are two coordi-

Table 1. Important bond lengths and bond angles of compound **1**.

Bond	Distance [Å]	Angle	[°]
Co1–N3	2.229(6)	N2–Co1–N3	99.6(2)
Co1–N4	2.231(5)	N3–Co1–N4	80.9(2)
Co1–N1	2.237(5)	N2–Co1–N1	81.3(2)
Co1–Cl1	2.3731(16)	N4–Co1–N1	98.2(2)
Co1–Cl2	2.3850(18)	Cl1–Co1–Cl2	178.81(7)
Co1–N2	2.213(5)		

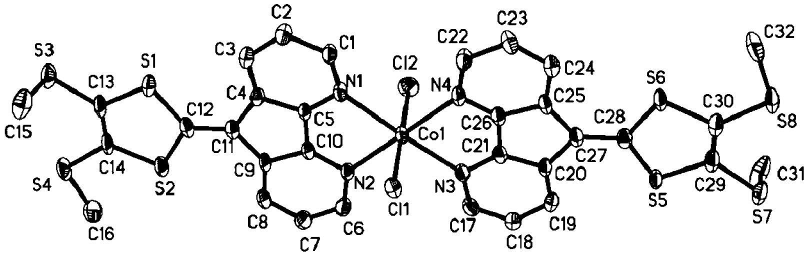

Figure 1. Crystal structure of compound **1** with the labeling scheme.

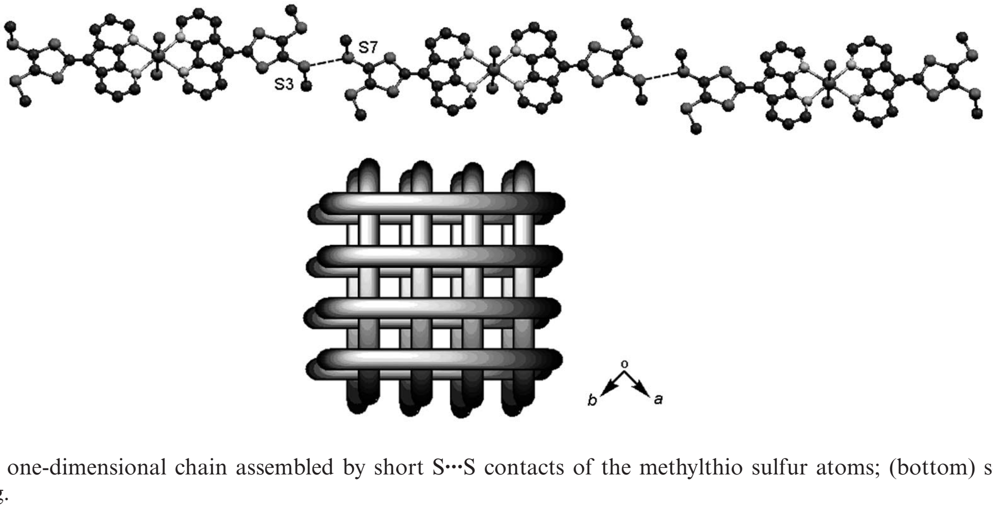

Figure 2. (top) A one-dimensional chain assembled by short S···S contacts of the methylthio sulfur atoms; (bottom) schematic view of the chain packing.

nated chlorine ions at *trans* axial positions. In the crystal structure of $[Mn(L^1)_2Cl_2]$,[11a] which is a Mn^{II} compound with a similar chemical formula to that of **1**, the coordinated chlorine ions occupy a *cis* position. In the structure of $[Mn(L^1)_2(H_2O)_2](ClO_4)_2$,[11a] the coordinated water molecules are also in the *trans* position. The mean deviations from the plane of the two L^1 ligands in **1** are 0.0211 and 0.0384 Å. The dihedral angle between the least-squares planes of the two L^1 ligands is 4.0°. So, the two L^1 ligands are almost coplanar. The bond lengths of Co1–N (2.213–2.237 Å) in compound **1** are somewhat longer than those of other cobalt complexes with ligands that include coordinated nitrogen atoms in the aromatic rings.[13–15]

In the crystal structure of **1**, short S···S contacts of 3.368 Å occur between two methylthio sulfur atoms of the neighboring molecules, which gives rise to a one-dimensional contacting chain (Figure 2, top). The chains are oriented in two different directions, and they are also alternately arranged to form a 3D contact network (Figure 2, bottom) with C···C contacts (3.309Å) between the L^1 planes and a Cl···H–C interaction between L^1 and the chloride anions.

$[Cd(L^1)_2(NO_3)_2]$ (2)

Compound **2** crystallizes in the orthorhombic system with four complex molecules in a unit cell. The X-ray crystal structure of compound **2** is shown in Figure 3 (top) and selected bond lengths and bond angles are listed in Table 2. The Cd^{II} ion is coordinated by four nitrogen atoms from two chelating ligands and two oxygen atoms from two *cis* nitrate anions that are disordered. The mean deviations from the plane of the two ligands are the same (0.0453 Å). The dihedral angle between the least-squares planes of the two ligands is 96.8°. The bond lengths Cd1–N1 2.416(4) Å and Cd1–N2 2.391(3) Å are similar to those of $[Cd(bipy)_2(NO_3)_2]$ (bipy = 2, 2′-bipyridine),[16] which is a Cd^{II} nitrate compound showing a coordination environment resembling that of compound **2**. The bond angle N1–Cd1–N2 75.42(13)° is larger than that of $[Cd(bipy)_2 (NO_3)_2]$, which is 69.8(4)°. The difference in the bond angle results from the different structures of the L^1 and bipy ligands. For example, the angle C10–C5–N1 is 124.2(4)°, whereas the corresponding one in bipy is 120°. The crystal is stabilized by interligand π–π stacking. The ligand planes from molecules having different symmetry are alternately arranged with C···C (3.372 Å) stacking and form 1D ligand columns along the *b* axis. By coordination of the metal, these π–π assembled ligand columns are further linked into a 2D structure that is parallel to the (001) plane (Figure 3, bottom). These characters are similar to those of $[Mn(L^1)_2(NO_3)_2]$,[11a] although their crystal systems are different.

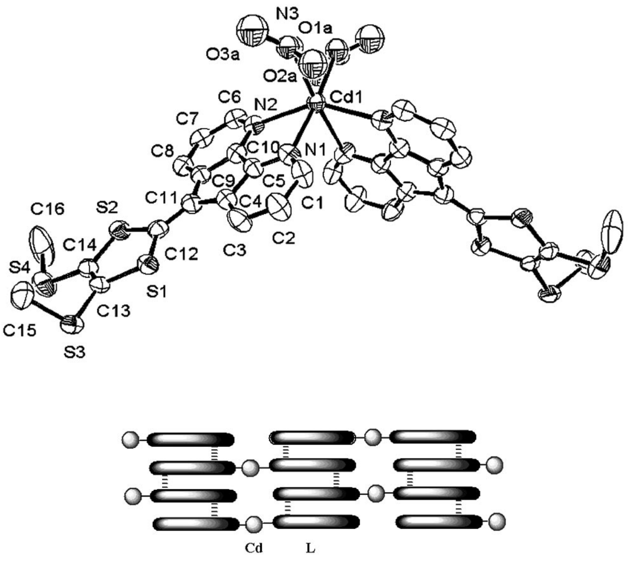

Figure 3. (top) Crystal structure of compound **2** with the labeling scheme; (bottom) schematic view of the molecular packing and intermolecular interactions.

Table 2. Important bond lengths and bond angles of compound **2**.

Bond	Distance [Å]	Angle	[°]
Cd1–O1A	2.228(6)	N2–Cd1–N2	148.67(17)
Cd1–O1B	2.343(11)	N2–Cd1–N1	75.42(13)
Cd1–N2	2.391(3)	N2–Cd1–N1	83.07(13)
Cd1–N1	2.416(4)	N1–Cd1–N1	92.84(18)
		N1–C5–C10	124.2(4)

$[Cu(L^2)_2Cl_2]\cdot CH_3OH\cdot 0.5(CH_2Cl_2)$ (3)

Compound **3** crystallizes in a monoclinic system with four complex molecules, four cocrystallized methanol molecules, and two dichloromethane molecules in a unit cell. The X-ray crystal structure of compound **3** is shown in Figure 4 (top) and selected bond lengths and bond angles are listed in Table 3. There are two different symmetrical molecules oriented in different directions, and they are [1,0,1] and [1,0,–1]. Because of the significant Jahn–Teller effect, the basic coordination environment around the copper centers is a square geometry, in which the Cu^{II} ion is coordinated by two nitrogen atoms from two L^2 ligands and two *trans*-coordinated chlorine ions. The other N atoms of the two ligands form two elongated weak bonds with the Cu^{II} ion in axial positions (the dashed bonds in Figure 4, top). The average distances of the Cu–N bonds are 2.694 Å in axial position and 2.000 Å in the square plane. Therefore, the coordination sphere of the Cu ions can also be considered as an elongated octahedral geometry. It is similar to that of $[Cu(dafone)_2Cl_2]$ (dafone = 4,5-diazafluoren-9-one),[17] which is a Cu^{II} chloride compound showing a coordination environment resembling that of compound **3**. The mean deviations from the plane of the two ligands are 0.046 and 0.899 Å. The dihedral angle between the least-squares planes of the two ligands is 3°. In the crystal structure of **3**, the ligand planes from two different symmetrical molecules are partly overlapped with C···C (3.322 Å) and C···S (3.498 Å) interactions, which forms a two-layer zigzag chain (Figure 4, bottom).

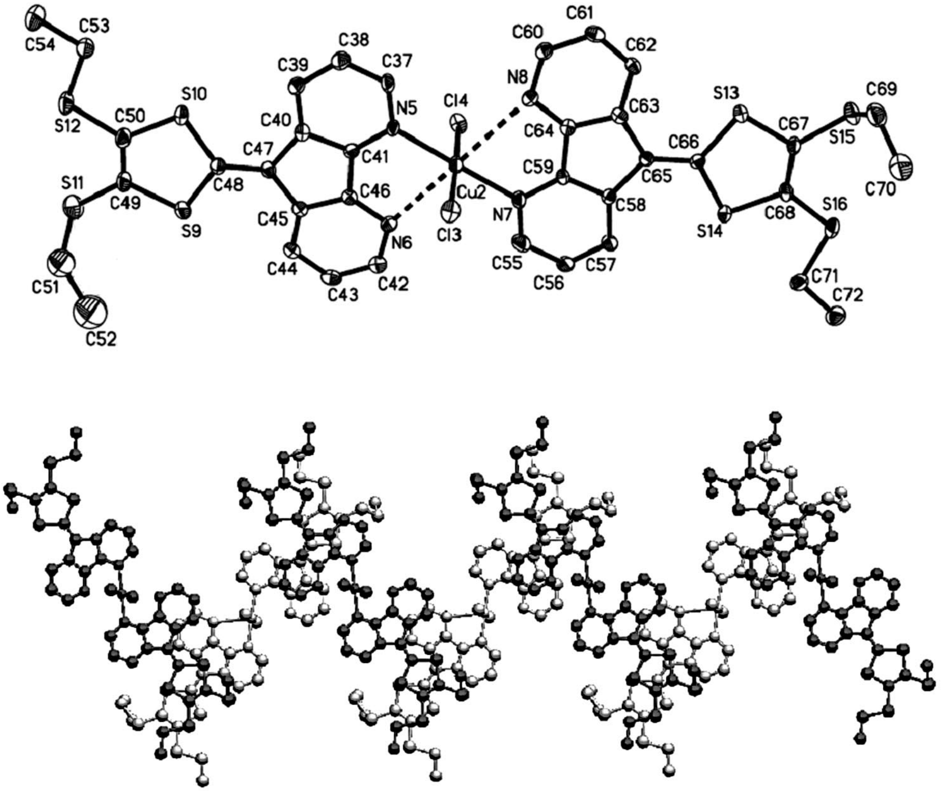

Figure 4. (top) Crystal structure of compound **3** with the labeling scheme; (bottom) A zigzag chain in which the ligand planes are partly overlapped with C···C (3.322 Å) and C···S (3.498 Å) interactions.

Table 3. Important bond lengths and bond angles of compound **3**.

Bond	Distance [Å]	Angle	[°]
Cu1–N1	1.971(5)	N1–Cu1–Cl1	90.97(19)
Cu1–N3	1.991(5)	N3–Cu1–Cl1	90.39(18)
Cu1–N2	2.711(5)	N3–Cu1–Cl2	88.57(18)
Cu1–N4	2.671(5)	N1–Cu1–Cl2	90.07(19)
Cu1–Cl1	2.288(2)	N1–Cu1–N2	77.54(18)
Cu1–Cl2	2.3135(19)	N3–Cu1–N4	77.71(18)
Cu2–N5	1.994(5)	N5–Cu2–Cl3	89.63(18)
Cu2–N7	2.001(5)	N7–Cu2–Cl3	89.46(19)
Cu2–N6	2.644(5)	N7–Cu2–Cl4	91.39(19)
Cu2–N8	2.749(5)	N5–Cu2–Cl4	89.59(19)
Cu2–Cl3	2.296(2)	N5–Cu2–N6	78.95(18)
Cu2–Cl4	2.307(2)	N7–Cu2–N8	76.27(18)

[Cu(L^2)$_2$Br$_2$]·CH$_3$OH (4)

Compound **4** crystallizes in the orthorhombic system with 16 complex molecules and 16 solvent methane molecules in a unit cell. The basic structure of **4** is the same as that of **3**, and selected bond lengths and bond angles are listed in Table 4. The copper(II) atom is surrounded in an N_2Br_2 square environment. Weak interactions from the N atoms of the L^2 ligands at the axial positions also exist, forming an elongated octahedron. It is similar to that of [Cu(dafone)$_2$Br$_2$] (dafone = 4,5-diazafluoren-9-one).[18] The bond lengths of the two axial interaction are 2.691 and 2.727 Å. The mean deviations from the plane of the two ligands are 0.0140 and 0.0770 Å. The dihedral angle between the least-squares planes of the two ligands is 3.8°.

Table 4. Important bond lengths and bond angles of compound **4**.

Bond	Distance [Å]	Angle	[°]
Cu1–N1	1.961(4)	N1–Cu1–N3	176.75(19)
Cu1–N3	1.969(4)	N1–Cu1–Br1	90.43(16)
Cu1–Br1	2.4727(11)	N1–Cu1–Br2	89.81(15)
Cu1–Br2	2.4603(11)	N3–Cu1–Br1	90.35(17)
		N3–Cu1–Br2	89.68(17)
		Br2–Cu1–Br1	175.17(4)

In the crystal structure of **4**, the short S···S contacts of 3.278 Å occur between two ethylthio sulfur atoms of the neighboring molecules, which are shorter than that in compound **1**. This indicates that there are strong interactions between two neighboring molecules, which give rise to a 1D chain. The packing of these chains in the crystal is similar to that of **1** (Figure 2, bottom), with efficient interactions of C···C (3.372 Å) and C···S (3.431 Å) between chains.

Absorption Spectra

The UV/Vis spectroscopic data of the L ligand and their complexes in dichloromethane were measured. A strong absorption band at about 410–415 nm appeared for the ligands. An intramolecular charge transfer, from dithiole to the bipyridine moieties (from π to π* transition), is attributed to the absorption. The representative spectra of L^1 and complex **1** are given in Figure 5. This absorption band at 414 nm for L^1 is redshifted slightly upon formation of the complex, especially in the slope on the lower energy side, which indicates that the coordination of a metal cation should turn the pyridine unit from a rather poor acceptor to a strong one. It suggests that the metal provides an enhancement of the pyridine withdrawing effect.

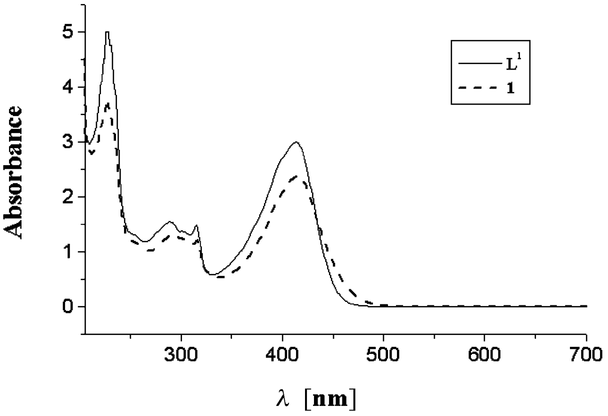

Figure 5. UV/Vis spectra of the L^1 ligand and compound **1** in dichloromethane.

The optical diffuse reflectance measurements were also carried out at room temperature. The absorption (a/S) data, in the range of 1.25 to 5 eV, were calculated from the reflectance by using the Kubelka–Munk function $a/S = (1 - R)^2/2R$.[19] The spectra of the L^1 ligand and compound **1** are displayed in Figure 6. The strong band at 3.0 eV (413 nm) corresponds to the intramolecular charge-transfer band found in solution. The coordination of the metal ion to the ligand causes a large redshift (2.8 eV; 443 nm) relative to that in solution. This means the intramolecular charge transition is enhanced in the solid state. Both the spectra of the ligand and compound **1** show steep absorption edges in the range of the intramolecular CT transition, which gives an initial optical transition obtained by extrapolation of the linear portion of the edges of 2.5 eV for the ligand and 2.1 eV for the complex. The weak bands at around 1.7 eV for complex **1** might be caused by coordination field transitions or intermolecular interactions in the solid state.

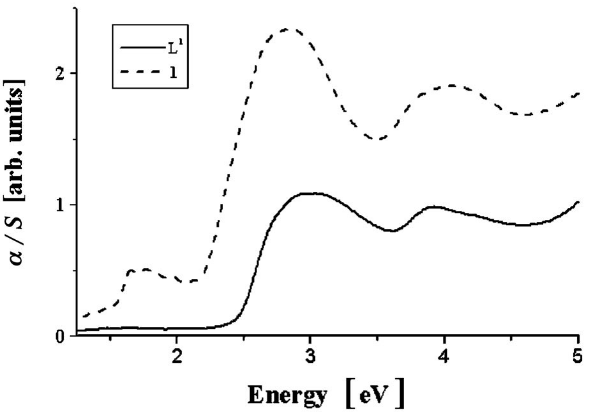

Figure 6. Solid-state optical absorption spectra of the L^1 ligand and compound **1**.

NLO Properties of the Compounds

The Z-scan technique has been used to study the third-order NLO properties. It is a single-beam method for measuring the optical nonlinearities by detecting the sample transmittance of a focused Gaussian beam as a function of the sample position (z). This method provides direct measurement of the real and imaginary parts of the nonlinearity, along with its sign, as well as nonlinear absorption and refraction. The sign of the nonlinearity is an important parameter for practical applications of optical signal processing devices. In Z-scan measurements, the intensity-dependent transmission of the sample measured without an aperture (open-aperture scan) gives information on purely absorptive nonlinearity, whereas the apertured scan (closed aperture) contains the information of both the absorptive and dispersive nonlinearities. The ratio of the normalized closed-aperture and open-aperture scans generates a Z scan due to the purely dispersive nonlinearity.

The Z-scan measurements in this work were carried out with a 1064-nm laser pulse of 7 ns duration in a THF solution of 1.67×10^{-4} mol dm^{-3} for compound **1**, 2.89×10^{-4} mol dm^{-3} for compound **2**, 1.95×10^{-4} mol dm^{-3} for compound **3**, and 1.14×10^{-4} mol dm^{-3} for compound **4**. As all the samples did not show the absorptive nonlinearity, the effective third-order NLO refractive effects were then assessed by the Z-scan data obtained under the closed-aperture configuration, and the NLO refractive index n_2 can be derived from Equation (1).[20]

$$n_2 = \frac{\lambda \alpha_0}{0.812 \pi I (1 - e^{-\alpha_0 L})} \Delta T_{V-P} \tag{1}$$

where ΔT_{V-P} is the difference between normalized transmittance values at valley and peak portion, I is the peak irradiation intensity at focus ($I_0 = 3.45 \times 10^{13}$ W m^{-2}), a_0 is the linear absorption coefficient, L is the sample thickness (2 mm in this study), and λ is the wavelength of the laser (1064 nm).

Curves a–d in Figure 7 depict the NLO refractive properties of compounds **1**–**4**, respectively. The valley/peak pattern of the normalized transmittance curve shows characteristic self-defocusing behavior. The data show that the four compounds have a similar negative sign for the refractive nonlinearity. Analysis of nonlinear optical systems with negative large γ values is interesting, as the systems possess intense electron correlation dependences and exhibit exceptional sensitivity with respect to subtle changes in the structures, namely, these systems are expected to be candidates for fundamental systems of "controllable nonlinear optical materials".[21] This self-defocusing behavior may be an advantage for the application in protection of optical sensors.

The difference in the valley/peak positions, ΔZ_{V-P}, and the difference between normalized transmittance values at valley and peak portions, ΔT_{V-P}, can be obtained from Figure 7. These data are listed in Table 5 with the calculated refractive index n_2. Nonlinear refractive indexes n_2 were reported for some best-performing NLO materials

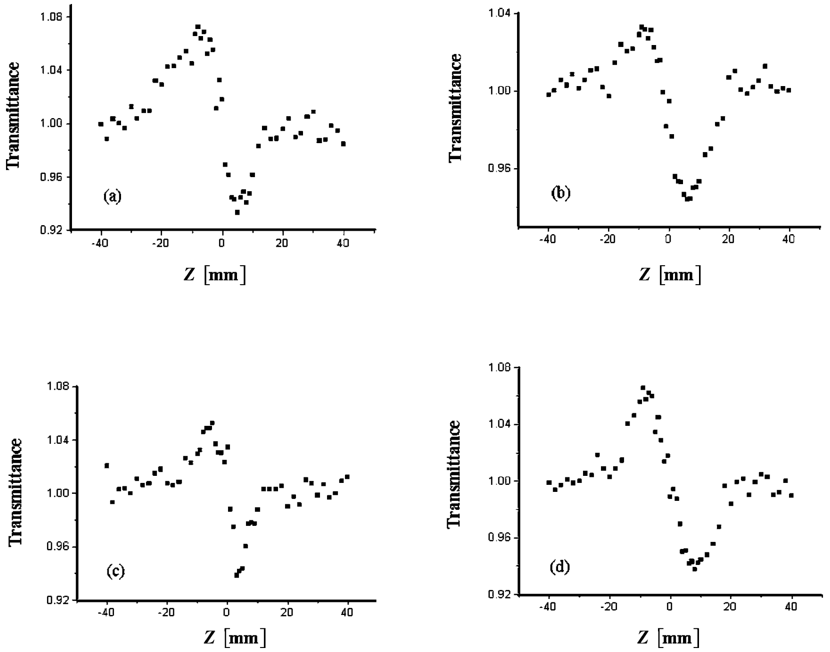

Figure 7. Z-scan data evaluated under closed-aperture configuration (a) compound **1** in 1.672×10^{-4} M THF; (b) compound **2** in 2.89×10^{-4} M THF; (c) compound **3** in 1.95×10^{-4} M THF; (d) compound **4** in 1.14×10^{-4} M THF.

such as semiconductors like CdS ($n_2 = 2.5\times10^{-18}\,\text{m}^2\text{W}^{-1}$), CdSe ($n_2 = -7.3\times10^{-19}\,\text{m}^2\text{W}^{-1}$), and GaAs ($n_2 = -1.6\times10^{-17}\,\text{m}^2\text{W}^{-1}$), and organic polymers like 4BCMU ($n_2 = 5\times10^{-18}\,\text{m}^2\text{W}^{-1}$), DANS ($n_2 = 8\times10^{-18}\,\text{m}^2\text{W}^{-1}$), and PTS ($n_2 = -2\times10^{-16}\,\text{m}^2\text{W}^{-1}$) as measured at 1.06 and 1.31 μm.[22] Even though the n_2 values of $-3.10\times10^{-18}\,\text{m}^2\text{W}^{-1}$, $-1.89\times10^{-18}\,\text{m}^2\text{W}^{-1}$, $-2.79\times10^{-18}\,\text{m}^2\text{W}^{-1}$, and $-2.47\times10^{-18}\,\text{m}^2\text{W}^{-1}$ in this paper were obtained with ca. 10^{-4} mol dm^{-3} THF solution, they match those of the best-known third-order NLO materials in neat solid form. Moreover, these values are also comparable to those of characteristic third-order NLO materials such as ferrocenyl complexes like $[\text{Ag(L)}_2](\text{NO}_3)\cdot(\text{MeOH})\cdot(\text{EtOH})$ ($n_2 = 1.15\times10^{-18}\,\text{m}^2\text{W}^{-1}$) and $[\text{HgI}_2\text{(L)}]$ ($n_2 = 8.02\times10^{-19}\,\text{m}^2\text{W}^{-1}$).[23]

In accordance with the n_2 values, the effective third-order NLO susceptibility $\chi^{(3)}$ values can be calculated by $\chi^{(3)} = cn_0^2n_2/80\pi$, where c is speed of light in a vacuum and n_0 is the linear refractive index of the sample. The $\chi^{(3)}$ values are also listed in Table 5. The corresponding modulus of the hyperpolarizability γ values were obtained from $\gamma = \chi^{(3)}/NF^4$, where N is the number density of a compound in the

Table 5. The $\chi^{(3)}_\text{R}$ and γ_R data for compounds **1**–**4** at a concentration of 2×10^{-4} M.

Compound	$\Delta Z_{\text{V–P}}$ [mm]	$\Delta T_{\text{V–P}}$	n_2 [m^{2}W^{-1}]	$\chi^{(3)}_\text{R}$ [m^{2}v^{-2}]	γ_R [m^{5}v^2]	[esu]
1	12	0.14	-3.10×10^{-18}	-2.18×10^{-20}	-6.98×10^{-44}	-5.0×10^{-30}
2	13	0.09	-1.89×10^{-18}	-1.33×10^{-20}	-2.45×10^{-44}	-1.8×10^{-30}
3	8	0.11	-2.79×10^{-18}	-1.96×10^{-20}	-9.21×10^{-44}	-6.6×10^{-30}
4	16	0.12	-2.47×10^{-18}	-1.73×10^{-20}	-4.76×10^{-44}	-3.4×10^{-30}

Table 6. The values of γ for some reported NLO materials.

Compound	γ [esu]	Ref.
$[\text{Et}_4\text{N}]_3[\text{WOS}_3(\text{CuI})_3(\mu_2\text{-I})]$	2.8×10^{-29}	[24]
$\text{WCu}_2\text{OS}_3(\text{PPh}_3)_4$	9.0×10^{-29}	[25]
C_{60}	7.5×10^{-34}	[26]
Ge	2.3×10^{-33}	[27]
Ferrocene	$(1.61\pm0.18)\times10^{-35}$	[28]
Group 10 metal alkynyl polymers	5.6×10^{-35} to 8.6×10^{-34}	[27,29]
Metallophalocyanines	1.0×10^{-32} to 1.0×10^{-31}	[30]
Octopolar alkynylruthenium complexes	9.3×10^{-35} to 3.6×10^{-33}	[31]
$[\text{Co(L}^1)_2\text{Cl}_2]\cdot2\text{CH}_3\text{OH}$ (**1**)	-5.0×10^{-30}	this work
$[\text{Cd(L}^1)_2(\text{NO}_3)_2]$ (**2**)	-1.8×10^{-30}	this work
$[\text{Cu(L}^2)_2\text{Cl}_2]\cdot\text{CH}_3\text{OH}\cdot0.5\text{CH}_2\text{Cl}_2$ (**3**)	-6.6×10^{-30}	this work
$[\text{Cu(L}^2)_2\text{Br}_2]\cdot\text{CH}_3\text{OH}$ (**4**)	-3.4×10^{-30}	this work

sample (in cm^{-3}) ($N = 10^{-3} \times CN_A$, C is the molar concentration of the compound in a THF solution, N_A is the Avogadro constant); F^4 is the local field correction factor. The calculated γ values for compounds **1**–**4** are -5.0×10^{-30}, -1.8×10^{-30}, -3.4×10^{-30}, and -6.6×10^{-30} esu, respectively (Table 5). Table 6 gives the γ values of some known NLO materials.[24–31] Most of the well-performing NLO materials reported in the literature are clusters, organic polymers, fullerene, semiconductors, and organometallic compounds. The γ values of complexes **1**–**4** are comparable to those of the known cluster compounds and are better than those of others. Hence, these systems are expected to be candidates for fundamental systems of controllable nonlinear optical materials. Although there seems to be no significant difference in the measurement results ($\gamma_R \approx 10^{-30}$ esu), the data for complex **1**, **3**, and **4** are larger than that of complex **2**. This means that the *trans* coordination of the two ligands to the metal center is beneficial to the third-order NLO properties, because of the coplanar structure of the two ligands in these compounds.

Conclusions

Four transition-metal complexes with the title ligands were synthesized, $[Co(L^1)_2Cl_2]·2CH_3OH$ (**1**), $[Cd(L^1)_2(NO_3)_2]$ (**2**), $[Cu(L^2)_2Cl_2]·CH_3OH·0.5CH_2Cl_2$ (**3**), $[Cu(L^2)_2Br_2]·CH_3OH$ (**4**), and their crystal structures were analyzed with respect to intermolecular interactions and the packing patterns. In compounds **1** and **4**, short S···S contacts exist between two alkylthio sulfur atoms of the neighboring molecules, and especially in compound **4**, there are strong S···S contacts (3.278 Å). Both the solution and solid-state electronic spectra show a redshift in the intramolecular charge-transfer bands upon formation of the metal complexes, which suggests that the metal coordination enhances the charge separation in the organic ligand. Their third-order nonlinear optical properties were studied, and the results show that these complexes exhibit negative γ values and are self-defocusing samples. The *trans* coordination of the two ligands to the metal center might be beneficial to the NLO properties due to their coplanar effect. The structural characterization and the measurement of the optical properties of the four compounds would be helpful to further understand the relationship between their structures and their optical properties.

Experimental Section

General Remarks: Elemental analyses of C, H, and N were measured with an EA1110 elemental analyzer. The IR spectra were recorded as KBr pellets with a Nicolet Magma 550 FTIR spectrometer. ^{1}H NMR spectra were measured with a UNITYNOVA-400 spectrophotometer. UV/Vis spectra were measured with a Shimadzu UV-3150 spectrometer at room temperature. The absorption (a/S) data were calculated from the reflectance by using the Kubelka–Munk function $a/S = (1 - R)^2/2R$, where R is the reflectance at a given energy, a is the absorption, and S the scattering coefficient. The third-order NLO properties of compounds **1**–**4** were measured by using the excitation provided by 7×10^{-9} s laser pulses at λ = 1064 nm.

Preparation of the Ligands: The ligands were synthesized by using a modified literature procedure.[32] A procedure for 4′,5′-diaza-9′-[4,5-bis(methylthio)-1,3-dithiol-2-ylidene]fluorene (L^1) is as follows: A solution of 4,5-diazafluoren-9-one (1.00 mmol, 0.1823 g) and 4,5-bis(methylthio)-1,3-dithiol-2-thione (1.2 mmol, 0.2720 g) in toluene (10 mL) was added to tributylphosphite (3.5 mL, 95%, 14.4 mmol), and the reaction mixture was heated at reflux for 4 h under an argon atmosphere. When cooled, a yellow precipitate was formed, which was filtered and washed with hexane. The crude product was purified by chromatography on a silica gel column (dichloromethane/methanol, 100:3). The final product, L^1, was recrystallized from chloroform. Yield: 0.1678 g (47%). M.p. >180 °C. IR (KBr): ṽ = 1540 (s), 1488 (s), 1393 (s), 1174 (s), 857 (m), 797 (m), 738 (m) cm^{-1}. ^{1}H NMR (400 MHz, CDCl$_3$): δ = 8.68 (dd, J = 1.1, 4.9 Hz, 2 H), 8.06 (dd, J = 1.2, 8.4 Hz, 2 H), 7.39 (dd, J = 5.0, 8.1 Hz, 2 H), 2.58 (s, 3 H) ppm. $C_{16}H_{12}N_2S_4$ (360.5): calcd. C 53.34, H 3.36, N 7.78; found C 53.28, H 3.40, N 7.69.

Ligand L^2 was synthesized by a similar method to that of L^1 by using 4,5-diazafluoren-9-one (1.00 mmol, 0.1823 g) and 4,5-bis(ethylthio)-1,3-dithiol-2-thione (1.2 mmol, 0.3048 g) as the starting materials to afford the final product L^2.Yield: 0.1520 g (40%). M.p. 162.0–162.5 °C. IR (KBr): ṽ = 1540 (s), 1480 (s), 1392 (s), 1173 (m), 856 (m), 802 (m), 745 (m) cm^{-1}. ^{1}H NMR (400 MHz, CDCl$_3$): δ = 8.68 (dd, J = 1.1, 4.9 Hz, 2 H), 8.07 (dd, J = 1.1, 8.2 Hz, 2 H), 7.39 (dd, J = 8.2, 4.6 Hz, 2 H), 3.02 (q, J = 7.4 Hz, 4 H), 1.41 (t, J = 7.3 Hz, 6 H) ppm. $C_{18}H_{16}N_2S_4$ (388.6): calcd. C 55.67, H 4.16, N 7.22; found C 55.56, H 4.10, N 7.16.

$[Co(L^1)_2Cl_2]·2CH_3OH$ (1): To a solution of $CoCl_2·6H_2O$ (0.01 mmol, 2.4 mg) in methanol (2 mL) was added a solution of ligand L^1 (0.02 mmol, 7.2 mg) in dichloromethane (5 mL). The mixture was stirred for 20 min at room temperature. By slowly evaporating the solution, the orange-red crystals suitable for X-ray diffraction were obtained after several days. Yield: 3.6 mg (39%). IR (KBr): ṽ = 1534 (s), 1474 (s), 1403 (m), 1173 (m), 870 (m), 810 (m), 741 (m) cm^{-1}. $C_{34}H_{32}Cl_2CoN_4O_2S_8$ (915.0): calcd. C 44.63, H 3.53, N 6.12; found C 44.73, H 3.40, N 6.29.

$[Cd(L^1)_2(NO_3)_2]$ (2): Orange crystals of **2** were obtained by a similar procedure to that of **1**. Yield: 3.4 mg (36%). IR (KBr): ṽ = 1535 (s), 1474 (s), 1403 (m), 1173 (m), 868 (m), 811 (m), 741 (m) cm^{-1}. $C_{32}H_{24}CdN_6O_6S_8$ (957.5): calcd. C 40.09, H 2.53, N 8.77; found C 40.10, H 2.60, N 8.67.

$[Cu(L^2)_2Cl_2]·CH_3OH·0.5(CH_2Cl_2)$ (3): Dark-green crystals of **3** were also prepared by a similar procedure to that of **1**. Yield: 4.1 mg (42%). IR (KBr): ṽ = 1535 (s), 1474 (s), 1397 (m), 1173 (m), 864 (m), 803 (m), 741 (m) cm^{-1}. $C_{37.5}H_{37}Cl_3CuN_4OS_8$ (986.1): calcd. C 45.78, H 3.79, N 5.70; found C 45.89, H 3.71, N 5.78.

$[Cu(L^2)_2Br_2]·CH_3OH$ (4): To a solution of $CuBr_2$ (0.01 mmol, 2.2 mg) in methanol (3 mL) was slowly added a solution of ligand L^2 (0.02 mmol, 7.6 mg) in dichloromethane (4 mL). The mixture was undisturbed for several days, and black crystals suitable for X-ray diffraction were obtained. Yield: 3.1 mg (30%). IR (KBr): ṽ = 1536 (s), 1474 (s), 1404 (m), 1173 (m), 867 (m), 803 (m), 741 (m) cm^{-1}. $C_{37}H_{36}Br_2CuN_4OS_8$ (1032.6): calcd. C 43.16, H 3.53, N 5.44; found C 43.19, H 3.47, N 5.52.

X-ray Crystallographic Study: X-ray Crystallographic data for complexes **1**–**4** were obtained by using a Rigaku Mercury CCD area detector with graphite-monochromated Mo-K_α (λ = 0.71073 Å) radiation. An empirical absorption correction was applied, and the structure was solved by the SHELXS97 software package. The re-

Table 7. The data of $\chi^{(3)}_{R}$ and γ_R for the compounds **1**–**4**.

	$C_{34}H_{32}Cl_2CoN_4O_2S_8$ (**1**)	$C_{32}H_{24}CdN_6O_6S_8$ (**2**)	$C_{37.5}H_{37}Cl_3CuN_4OS_8$ (**3**)	$C_{37}H_{36}Br_2CuN_4OS_8$ (**4**)
Formula weight	914.95	957.45	986.08	1032.54
Dimensions [mm]	0.40 × 0.30 × 0.19	0.30 × 0.25 × 0.20	0.45 × 0.30 × 0.20	0.43 × 0.42 × 0.25
Crystal system	monoclinic	orthorhombic	monoclinic	orthorhombic
Space group	*C*2	aba2	P21	fdd2
a [Å]	20.854(3)	14.023(3)	16.3930(18)	33.187(3)
b [Å]	16.767(2)	28.941(5)	14.1551(12)	35.804(3)
c [Å]	14.500(2)	9.1065(17)	18.480(2)	13.9351(12)
β [°]	125.612(3)	90	90.784(3)	90.00
V [Å^3]	4121.7(11)	3695.7(11)	4287.7(8)	16558(3)
T [K]	193(2)	193(2)	193(2)	193(2)
Z	4	4	4	16
$D_{\text{calcd.}}$ [g cm^{-3}]	1.474	1.721	1.528	1.657
μ [mm^{-1}]	0.988	1.097	1.123	2.898
F(000)	1876	1928	2024	8336
Reflections (total)	7491	3369	15206	7545
Reflections (gt)	6656 ($I > 2\sigma I$)	3244 ($I > 2\sigma I$)	11760 ($I > 2\sigma I$)	7141 ($I > 2\sigma I$)
R_1(gt)	0.0557	0.0337	0.0588	0.0442
wR_2 (gt)	0.1701	0.0834	0.1469	0.1038
Goodness of fit	1.097	1.065	1.000	1.052

finement was performed against F^2 by using SHELXL-97. All non-hydrogen atoms were refined anisotropically. The hydrogen atoms were positioned with idealized geometry and refined with fixed isotropic displacement parameters. The oxygen atoms of the nitrate anions in **2** are disordered and the occupancies of A/B were assigned as 66 and 34%, respectively. The solvent molecules (MeOH) in **1** and **4** and one ethylthio group of **3** are also disordered. The H atoms of the disordered atoms were not dealt with. Table 7 lists relevant crystallographic data for complex **1**–**4** and details of data collection.

CCDC-649852, -649853, -649854, and -649855 contain the supplementary crystallographic data for this paper. These data can be obtained free of charge from The Cambridge Crystallographic Data Centre via www.ccdc.cam.ac.uk/data_request/cif.

Nonlinear Optical Measurements: The NLO properties of a solution of the sample in THF were determined by using a standard Z-scan setup with a Q-switched Nd:YAG laser (pulse widths = 7 ns, I_0 = 3.45×10^{13} W m^{-2}). The pulse-repetition rate was 10 Hz. The transmittance of the aperture in front of the detector for a closed-aperture measurement was 0.1. The solution was contained in a 2-mm thick quartz cell.

Acknowledgments

This work was supported by the NNS Foundation (20371033) and the NSF of the Education Committee of Jiangsu Province (06KJB150102), P.R. China.

---

[1] P. G. Lacroix, R. Clèment, K. Nakatani, J. Zyss, I. Ledoux, *Science* **1994**, *263*, 658–660.

[2] P. G. Lacroix, K. Nakatani, *Adv. Mater.* **1997**, *9*, 1105–1108.

[3] R. Andreu, I. Malfant, P. G. Lacroix, H. Gornitzka, *Chem. Mater.* **1999**, *11*, 840–848.

[4] R. H. Friend, R. W. Gymer, A. B. Holmes, J. H. Burroughes, R. N. Marks, C. Taliani, D. D. C. Bradly, D. A. dos Santos, J. L. Brédas, M. Lögdlung, W. R. Salaneck, *Nature* **1999**, *397*, 121–128.

[5] Q. Wang, L. Yu, *J. Am. Chem. Soc.* **2000**, *122*, 11806–11811.

[6] a) S. R. Marder, D. W. Bruce, D. O'Hare (Eds.), *Inorganic Materials*, Wiley, Chichester, **1992**, p. 115; b) N. J. Long, *Angew. Chem. Int. Ed. Engl.* **1995**, *34*, 21–38.

[7] D. W. Bruce, D. O'Hare (Eds.), *Inorganic Materials*, 2nd ed., John Wiley & Sons, Chichester, **1996**, pp. 122–169.

[8] a) N. Robertson, L. Cronin, *Coord. Chem. Rev.* **2002**, *227*, 93–127; b) E. I. Stiefel (Ed.), "Dithiolene Chemistry, Syntheses, Properties and Applications" in *Progress in Inorganic Chemistry*, Wiley, New York, **2004**, vol. 52.

[9] a) S. A. Baudron, M. W. Hosseini, *Inorg. Chem.* **2006**, *45*, 5260–5262; b) S. A. Baudron, M. W. Hosseini, N. Kyritsakas, *New J. Chem.* **2006**, *30*, 1083–1086; c) S. A. Baudron, M. W. Hosseini, N. Kyritsakas, M. Kurmoo, *Dalton Trans.* **2007**, 1129–1139.

[10] a) J. Vicente, P. González-Herrero, Y. García-Sánchez, *Inorg. Chem.* **2004**, *43*, 7516–7531; b) J. Vicente, P. González-Herrero, M. Pérez-Cadenas, P. G. Jones, D. Bautista, *Inorg. Chem.* **2005**, *44*, 7200–7213; c) J. Vicente, P. González-Herrero, Y. García-Sánchez, P. G. Jones, D. Bautista, *Eur. J. Inorg. Chem.* **2006**, 115–126; d) J. Vicente, P. González-Herrero, M. Pérez-Cadenas, *Inorg. Chem.* **2007**, *46*, 4718–4732.

[11] a) Q. Y. Zhu, J. Dai, D. X. Jia, L. H. Cao, H. H. Lin, *Eur. J. Inorg. Chem.* **2004**, 4789–4794; b) Q. Y. Zhu, Y. Zhang, J. Dai, G. Q. Bian, D. X. Jia, J. S. Zhang, L. Guo, *Chem. Lett.* **2003**, *32*, 762–763; c) Q. Y. Zhu, G. Q. Bian, J. Dai, D. X. Jia, J. S. Zhang, L. Guo, *Inorg. Chim. Acta* **2003**, *351*, 177–182.

[12] a) C. S. Winter, C. A. S. Hill, A. E. Underhill, *Appl. Phys. Lett.* **1991**, *58*, 107–109; b) S. F. Wang, W. T. Huang, T. Q. Zhang, Q. H. Gong, Y. Okuma, M. Horikiri, Y. F. Miura, *Appl. Phys. Lett.* **1999**, *75*, 1845–1847; c) X. B. Sun, X. Q. Wang, Q. Ren, G. H. Zhang, H. L. Yang, L. Feng, *Mater. Res. Bull.* **2006**, *41*, 177–182.

[13] W. Henke, S. Kremer, D. Reinen, *Z. Anorg. Allg. Chem.* **1982**, *491*, 124–136.

[14] D. R. Zhu, Y. Song, Y. Xu, Y. Zhang, S. S. S. Rai, H. K. Fun, X. Z. You, *Polyhedron* **2000**, *19*, 2019–2025.

[15] G. de Munno, T. Poeiro, M. Julve, F. Lloret, G. Vlau, *New J. Chem.* **1998**, *22*, 299–305.

[16] P. F. Rodesiler, R. W. Turner, N. G. Charles, E. A. H. Griffith, E. L. Amma, *Inorg. Chem.* **1984**, *23*, 999–1004.

[17] C. Balagopalakrishna, M. V. Rajasekharan, S. Bott, J. L. Atwood, B. L. Ramakrishna, *Inorg. Chem.* **1992**, *31*, 2843–2846.

[18] S. Menon, M. V. Rajasekharan, *Polyhedron* **1998**, *17*, 2463–2476.

[19] W. W. Wendlandt, H. G. Hecht, *Reflectance Spectroscopy*, Interscience Publishers, New York, **1966**.

[20] a) M. Sheik-Bahae, A. A. Said, E. W. V. Stryland, *Opt. Lett.* **1989**, *14*, 955–957; b) M. Sheik-Bahae, A. A. Said, T. H. Wei,

D. J. Hagan, E. W. V. Stryland, *IEEE J. Quantum Electron.* **1990**, *26*, 760–769.

[21] M. Nakano, S. Yamada, K. Yamaguchi, *Chem. Phys. Lett.* **1996**, *251*, 381–386.

[22] a) J. L. Bredas, C. Adant, P. Tackx, A. Persoons, B. M. Pierce, *Chem. Rev.* **1994**, *94*, 243–278; b) R. Adair, L. L. Chase, S. A. Payne, *Phys. Rev. B: Condens. Matter* **1989**, *39*, 3337–3349; c) M. Sheik-Bahae, D. C. Hutching, D. J. Hagan, E. W. Van Stryland, *IEEE J. Quantum Electron.* **1991**, *27*, 1296–1309.

[23] H. W. Hou, G. Li, Y. L. Song, Y. T. Fan, Y. Zhu, L. Zhu, *Eur. J. Inorg. Chem.* **2003**, 2325–2332.

[24] H. W. Hou, B. Liang, X. Q. Xin, K. B. Yu, P. Ge, W. Ji, S. Shi, *J. Chem. Soc. Faraday Trans.* **1996**, *92*, 2343–2346.

[25] S. Shi, H. W. Hou, X. Q. Xin, *J. Phys. Chem.* **1995**, *99*, 4050–4053.

[26] Y. Wang, L. T. Cheng, *J. Phys. Chem.* **1992**, *96*, 1530–1532.

[27] S. Guha, C. C. Frazier, P. L. Porter, K. Kang, S. Finberg, *Opt. Lett.* **1989**, *14*, 952–955.

[28] S. Ghosal, M. Samoc, P. N. Prasad, J. J. Tufariello, *J. Phys. Chem.* **1990**, *94*, 2847–2851.

[29] W. J. Blau, H. J. Byrne, D. J. Cardin, A. P. Davey, *J. Mater. Chem.* **1991**, *1*, 245–249.

[30] J. S. Shirk, J. R. Lindle, F. J. Bartoli, Z. H. Kafafi, A. W. Snow in *Materials for Nonlinear Optics* (Eds.: S. R. Marder, J. E. Sohn, G. D. Stucky), American Chemical Society, Washington, DC, **1992**, p. 626.

[31] A. M. McDonagh, M. G. Humphrey, M. Samoc, B. Luther-Davies, S. Houbrechts, T. Wadw, H. Sasabe, A. Persons, *J. Am. Chem. Soc.* **1999**, *121*, 1405–1406.

[32] K. Sako, M. Kusakabe, H. Tatemitsu, *Mol. Cryst. Liq. Cryst.* **1996**, *285*, 101–106.

Received: August 18, 2007